

Chapter 3

A Single-Molecule Barcoding System using Nanoslits for DNA Analysis: Nanocoding

Kyubong Jo, Timothy M. Schramm, and David C. Schwartz

Summary

Single DNA molecule approaches are playing an increasingly central role in the analytical genomic sciences because single molecule techniques intrinsically provide *individualized* measurements of selected molecules, free from the constraints of bulk techniques, which blindly average noise and mask the presence of minor analyte components. Accordingly, a principal challenge that must be addressed by all single molecule approaches aimed at genome analysis is how to immobilize and manipulate DNA molecules for measurements that foster construction of large, biologically relevant data sets. For meeting this challenge, this chapter discusses an integrated approach for microfabricated and nanofabricated devices for the manipulation of elongated DNA molecules within nanoscale geometries. Ideally, large DNA coils stretch via nanoconfinement when channel dimensions are within tens of nanometers. Importantly, stretched, often immobilized, DNA molecules spanning hundreds of kilobase pairs are required by all analytical platforms working with large genomic substrates because imaging techniques acquire sequence information from molecules that normally exist in free solution as unrevealing random coils resembling floppy balls of yarn. However, nanoscale devices fabricated with sufficiently small dimensions fostering molecular stretching make these devices impractical because of the requirement of exotic fabrication technologies, costly materials, and poor operational efficiencies. In this chapter, such problems are addressed by discussion of a new approach to DNA presentation and analysis that establishes scaleable nanoconfinement conditions through reduction of ionic strength; stiffening DNA molecules thus enabling their arraying for analysis using easily fabricated devices that can also be mass produced. This new approach to DNA nanoconfinement is complemented by the development of a novel labeling scheme for reliable marking of individual molecules with fluorochrome labels, creating molecular barcodes, which are efficiently read using fluorescence resonance energy transfer techniques for minimizing noise from unincorporated labels. As such, our integrative approach for the realization of genomic analysis through nanoconfinement, named nanocoding, was demonstrated through the barcoding and mapping of bacterial artificial chromosomal molecules, thereby providing the basis for a high-throughput platform competent for whole genome investigations.

Key words: DNA labeling, Genomics, Nanofabrication, Polymer confinement, Low ionic strength, FRET, Nicking enzyme, Physical mapping

1. Introduction

The explosion of single molecule approaches and microfluidics offers promising routes for effectively dealing with real-world biological applications requiring large data sets. Advances in this direction have stemmed from the appreciation of polymer behavior exhibited within typical microfluidic devices that have laid the basis for the development of practical approaches for molecular presentation. However, taking new theoretical insights forward for the development of practical genome analysis systems built around microfluidic and nanofluidic devices has proven difficult. Consider that most previously described microfluidic devices lack functionalities required for the large-scale manipulation of very large DNA molecules typically extracted from cells as genomic substrates. In addition, few devices have been specifically designed for operation within an integrated system—a necessary step if any device is to be used for meaningful application as a platform genomic analysis.

In this regard, Optical Mapping (*1*) is an unique high-throughput system using microfluidic devices designed to manipulate ensembles of very large genomic DNA molecules with sequence-specific decoration (*2, 3*). With the Optical Mapping system, a solution of DNA molecules flows in microfluidic channels via capillary force, elongating then depositing individual molecules in the same orientation on a positively charged surface via electrostatic interactions, creating massive single molecule arrays. These electrostatic interactions are strong enough that the molecules are held to the surface in an elongated fashion yet remain viable biochemical substrates (*4, 5*). After individual DNA molecules are presented as arrays, restriction enzyme action recognizes and cleaves specific sequences along the DNA backbones for generating discrete DNA restriction fragments that remain ordered on the surface. Subsequent staining with fluorochrome dyes that bind DNA enable fluorescence microscopy to rapidly image and analyze molecules using a fully automated system. Image analysis software identifies DNA molecule backbones, determines the size of each daughter restriction fragment, and generates one physical map (ordered restriction map) per molecule. Consensus maps are constructed from many single molecule maps using dedicated algorithms (*6, 7*) for subsequent biological analysis, such as useful scaffolds for guiding sequence assembly (*8–11*), comparative genomic studies (*12*), and the discovery of genomic structural alterations or “differences” involving kilobase- to megabase-sized changes in human genomes (*3, 6*).

Direct analysis of individual DNA molecules for genome analysis has been realized through the development of Optical Mapping. Nevertheless, a principal challenge faced using single molecule approaches is still the immobilization of a large number of samples,

yet maintenance of competent biochemical activity. For example, fixation of elongated DNA molecules on positively charged surfaces suffers from a range of shortcomings that molecules in free solution can obviate. In this regard, the optimum approach for substrate immobilization is no immobilization; the best chemical linker is no chemical linker. As such, entropic confinement techniques offer a uniquely powerful route to purely physical means for immobilization, which can be realized through the nanofabrication of features that leverage the wonderfully facile entropic properties of large coils such as DNA (13–15). The “stiffness” of double-stranded DNA and the long polymer length provide ample opportunities through entropic confinement techniques (16).

This chapter describes a single-molecule system using nanoconfinement for genomic analysis using disposable nanoscale silicone rubber devices and chemistries that reproducibly elongate large DNA molecules by 60% of their polymer contour length in concert with a single DNA molecule labeling scheme possessing low-noise characteristics. This approach facilitates the development of a truly high-throughput system for genomic analysis.

2. Materials

2.1. Fabrication of Master Wafer

1. Chrome mask array pattern of 750 nm × 5 mm (Center for Nanotechnology of the University of Wisconsin-Madison, Madison, WI).
2. Photoresist SU-8 2000.5 for nanoslits and SU-8 2005 for microchannel overlay (Microchem, Newton, MA).
3. Reactive ion etching instrument (Unaxis 790 RIE, Unaxis Wafer Processing, St. Petersburg, FL).
4. Piranha: 80% H₂SO₄ and 20% H₂O₂. Extremely corrosive. Wear proper eye/hand/body protection.
5. Alpha step 200 profilometer (KLA-Tencor, San Jose, CA).

2.2. PDMS Nanoslit Preparation

1. Polydimethylsiloxane (PDMS, Sylgard 184, Dow Corning, Midland, MI).
2. Oxygen plasma chamber (Technics Plasma GmbH 440, Technics Plasma GmbH, Florence, KY).
3. Ethylenediamine tetraacetic acid (EDTA, 0.5 M) adjusted to pH 8.5.

2.3. Clean Glass Preparation

1. Coverslips (22 mm × 22 mm) (Fischer Scientific, Pittsburgh, PA).
2. Nano-Strip (sulfuric acid and hydrogen peroxide) (Cyantek Corp., Fremont, CA). Extremely corrosive. Wear proper eye/hand/body protection.

3. Concentrated hydrochloric acid (12 M). Wear proper eye/hand/body protection.

2.4. DNA Barcoding

All concentrations listed are final; stocks that are more concentrated need to be made and diluted in the reaction solution to final concentration.

1. Bacterial artificial chromosomes (BAC) 79, 150, 614 from *E. coli* K-12; any BAC clone will suffice.
2. NEBuffer 2: 50 mM NaCl, 10 mM Tris-HCl, 10 mM MgCl₂, 1 mM dithiothreitol, pH 7.9 (New England Biolabs, Ipswich, MA).
3. NEBuffer 4: 50 mM potassium acetate, 20 mM Tris-acetate, 10 mM magnesium acetate, 1 mM dithiothreitol, pH 7.9 (New England Biolabs).
4. Restriction enzymes FseI and SpeI (New England Biolabs).
5. T4 DNA ligase (New England Biolabs).
6. 1 mM ATP to be used as a cofactor for T4 DNA ligase (Sigma-Aldrich).
7. Nicking enzyme: Nb.BbvCI (New England Biolabs).
8. Deoxyribonucleotides (dNTP): dATP, dCTP, dGTP, dTTP (New England Biolabs). 20 μ M solutions of each were made in Tris-EDTA buffer (TE).
9. Alexa Fluor 647-aha-dCTP and Alexa Fluor 647-aha-dUTP (Invitrogen) were prepared as 2 μ M solutions in TE. Protect from light.
10. *E. coli* DNA polymerase I, endonuclease-free grade (Roche Applied Sciences, Indianapolis, IN).
11. Dideoxyribonucleotides (ddNTP): ddATP, ddCTP, ddGTP, ddTTP (Amersham Biosciences, Piscataway, NJ) prepared as 0.2 μ M each in TE.
12. Proteinase K (Bioline, Taunton, MA).
13. *n*-Lauroyl sarcosine (Sigma-Aldrich, St. Louis, MO).
14. Micro dispodialyzer (Spectrum Laboratories, Rancho Dominguez, CA).

2.5. DNA Sample Preparation in Low Ionic Strength and Loading

1. DNA of bacteriophage λ (48.5 kbp) from New England Biolabs. Stock concentration of 500 ng/ μ L, final concentration 1 ng/ μ L.
2. DNA of bacteriophage T4 (166 kbp) from Waco Chemicals USA, which is the vendor of Nippon Gene, Japan. Stock concentration of 390 ng/ μ L, diluted to final concentration of 0.78 ng/ μ L.
3. YOYO-1 from Invitrogen, Inc. (Eugene, OR). Final concentration of 0.25 μ M from stock, which is 1 mM in DMSO. Protect from light.

4. β -mercaptoethanol as an antibleaching agent from Sigma-Aldrich.
5. Tris-EDTA buffer (1 \times TE): 10 mM Tris-HCl and 1 mM EDTA, pH 8.0. Tris EDTA buffer is made as follows: Tris base and EDTA acid are dissolved together, and titrated to pH 8.0 with HCl (*see Note 1*).
6. POP6 (Applied Biosystems, Foster City, CA).

2.6. Microscopy and Image Processing

1. Argon ion laser (488 nm; Spectra Physics 2017, Spectra Physics Laser Inc., Irvine, CA).
2. Inverted Microscope (Zeiss 135M equipped with a 63 \times Zeiss Plan-Neofluor oil immersion objective, Carl Zeiss Inc., Jena, Germany) (2).
3. Charge-coupled device digital camera (CCD, Hamamatsu ORCA-ER, 1344 \times 1024 pixels, 12-bit digitization, Hamamatsu Photonics Inc., Hamamatsu, Japan) and Cooke Pixelfly CCD cameras (1,376 \times 1,040, 12-bit, Applied Scientific Instrumentation, Eugene, OR).
4. Emission filters for the green channel (XF3086) and for the red channel (XF3076) (Omega Optical, Inc., Brattleboro, VT).
5. All software programs from image collection to image analysis are written in our laboratory. For microscopy and image collection, programs are written in Borland C++ Builder 6.0 (Cupertino, CA) and, for image analysis, programs are written in C++ using GTK and GNOME library in the Linux system.

3. Methods

3.1. Fabrication of Master Wafer

1. Prepare a chrome mask of 750 nm \times 5-mm array fabricated by e-beam lithography.
2. Spin coat a negative photoresist (SU-8 2000.5) onto a silicon wafer.
3. Illuminate the silicon wafer through the chrome mask to create arrays of 1- μ m-wide, 5-mm-long slits (*see Note 2*).
4. Etch the wafer 100 nm deep using a reactive ion etching (RIE) machine with CF₄ at 10 mTorr for 8 min (*see Note 3*).
5. Clean the etched wafer using piranha solution to lift off the photoresist layer (SU-8 2000.5).
6. Measure the height of the nanoslits (100-nm high \times 1- μ m wide) using an alpha step profilometer and measure the width under a scanning electron microscope (*see Fig. 1d*).
7. Overlay a microchannel array (3- μ m high, 100- μ m wide, and 10-mm long) on the nanopatterned wafer using the negative

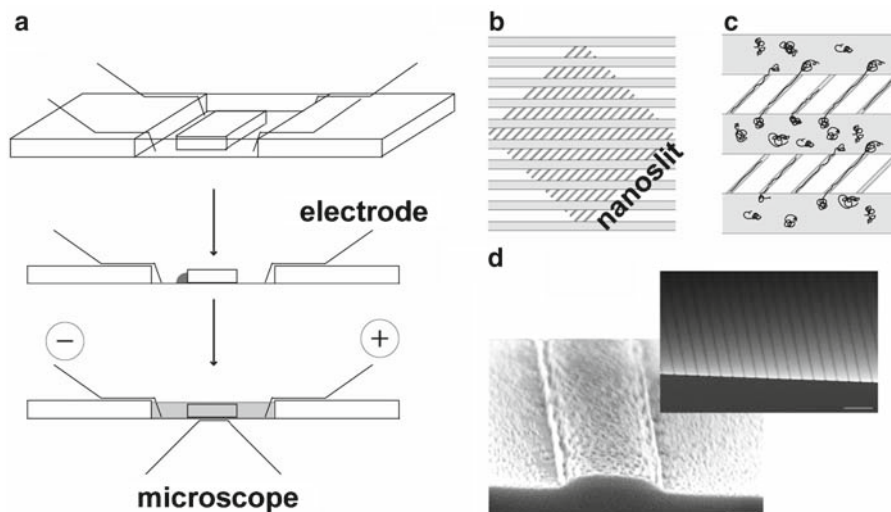


Fig. 1. The micro nanoslit device design and loading scheme. **(a)** For microscopy, a small chamber is fashioned from a Plexiglas™ slide (25.4×76.2 mm) with a rectangular opening to which a glass coverslip window (18×18 mm) is affixed with wax. The PDMS device is adhered to the coverslip window within the chamber. Pipetting applies DNA solution to microchannels, loading into the device by capillary action and then a buffer solution is added for electrokinetic loading. **(b)** Illustration (*top view*) shows nanoslits (diagonal; 100-nm high \times 1,000-nm wide) overlaid with microchannels (horizontal; 3- μ m high \times 100- μ m wide). **(c)** Cartoon depicts relaxed and elongated DNA molecules as occurring during electrokinetic loading within the microchannels and nanoslits, respectively. **(d)** Scanning electron micrograph of the silicon master shows a single nanoslit mold feature (bar = 300 nm); inset image shows many such nanoslit features spaced 4- μ m apart (center-to-center; bar = 10 μ m) (Reproduced from ref. (16). Copyright 2007 National Academy of Sciences, USA).

photoresist SU-8 2005 in the second cycle of photolithography (*see Fig. 1b*). The mask for the second cycle is a transparency film drawn in AutoCAD 2002 (<http://www.autodesk.com/autocad>).

8. Perform vapor deposition of tridecafluoro-1,1,2,2-tetrahydro octyl-trichloro silane for silanization of the patterned wafer to promote PDMS releasing (17). Place a patterned wafer in a Petri dish, add a drop of coating chemical at the corner of the Petri dish, close, and allow for vapor to deposit for an hour.

3.2. PDMS Nanoslit Preparation

1. Mix PDMS prepolymer with catalyst in a 10:1 ratio for 10 min.
2. Pour PDMS onto the silicon wafer master contained in a Petri dish.
3. Cure PDMS at 65°C for longer than 24 h, and peel it from the master wafer (*see Note 4*).
4. Perform oxygen plasma treatment in the Technics Plasma GmbH 440 to make the PDMS surface hydrophilic (O_2 pressure, ~ 0.67 millibars; load coil power, 100 W; 36 s).
5. Store plasma-treated devices in high-purity water for 24 h (*see Note 5*).

6. Sonicate the PDMS devices in a 50-mL conical tube filled with 0.5 M EDTA (pH 8.5) for 15 min to extract platinum (II) ions (*see Note 6*).
7. Sonicate the PDMS devices thoroughly in a 50-mL conical tube filled with high-purity water three times for 15 min each and store in high-purity water.
8. Dry the PDMS devices before use.

3.3. Clean Glass Preparation

Cleaning glass surfaces follows the cleaning procedure for Optical Mapping surfaces (3, 18, 19) (*see Note 7*). Heating concentrated acids can be dangerous and great care should be taken when executing this procedure. Proper eye/hand/skin protection must be used and the procedure must be done in a fume hood to avoid noxious vapors.

1. Fit cover slips (22 × 22 mm) in a Teflon rack and wrap with Teflon tape to hold them securely.
2. Set Teflon racks in a Pyrex glass cylinder (*see Note 7*).
3. Heat coverslips in Nano-Strip for 50 min after reaching 70°C. Allow for the cylinders to cool before draining the Nano-Strip.
4. Rinse the cylinder meticulously six times with high-purity and dust-free water.
5. Pour hydrochloric acid into the cylinder; make sure to cover the top of the Teflon rack by a few inches because some volume will be lost during boiling.
6. Boil in hydrochloric acid solution for 6 h once the liquid reaches 104°C to impart a uniform hydrolysis of the glass surface.
7. Rinse extensively with high-purity water to a neutral pH.
8. Remove the cover slips from the Teflon racks one at a time, and rinse them three times in absolute ethanol.
9. Store the clean coverslips under absolute ethanol in polypropylene containers at room temperature.

3.4. DNA Barcoding

All concentrations are final concentrations.

1. Linearize DNA molecules using a one-cut restriction enzyme if they are circular. FseI was used to linearize BAC79 and BAC150; SpeI for BAC614 (*see Note 8*).
2. Add 2 U T4 DNA ligase at 16°C for 2 h in 17.5 µL of NEBuffer 2 or 4 to attenuate indigenous nicks (*see Note 9*).
3. Inactivate T4 DNA ligase at 65°C for 10 min.
4. To the DNA solution, add 10 U *E. coli* DNA polymerase I and 0.2 µM ddNTPs at 37°C for 30 min in 40 µL in NEBuffer 2 or 4 to block remaining nicks (*see Notes 10 and 11*).

5. Add the labeling reaction mix of 20 U Nb.BbvCI, 2 μ M Alexa Fluor 647-aha-dCTP, 2 μ M Alexa Fluor 647-aha-dUTP, 20 μ M dATP, 20 μ M dGTP, 1 μ M dCTP, and 1 μ M dTTP (*see Note 12*)."
6. Incubate the mix for 30 min at 37°C.
7. Stop the reaction by adding 20 μ M EDTA, pH 8.5.
8. Digest enzymes by adding proteinase K to a final concentration of 100 ng/ μ L and *n*-lauroyl sarcosine to 0.1%, w/v and incubating for 3 h at 50°C.
9. Adjust buffer conditions by simple dilution with water (~2,000–4,000 times) or dialysis against 500 mL of 100 μ M Tris and 10 μ M EDTA (pH 8.0; 0.01 \times TE) buffer solution overnight with micro dispoalyzer at 4°C.

3.5. DNA Sample Preparation in Low Ionic Strength and Loading

Figure 2 shows images of electrokinetically loaded λ DNA (48.5 kbp), T4 DNA (166 kbp), and fragments of *E. coli* genomic DNA. To form these elongated single DNA molecules, a molecule undergoes electrophoresis within a microchannel toward a nanoslit entrance, where it proceeds to enter, and then stretch. Low ionic-strength solution facilitates the stretching of DNA molecules within nanoslits.

1. Prepare low ionic-strength buffer by adding high-purity water. An example is demonstrated in **Fig. 3**, where 1 \times TE buffer is diluted by 5-, 10-, 15-, 20-, 50-, or 100-fold with water. To the dilutions of TE, add intercalating dye YOYO-1 (0.25 μ M, final), antibleaching agent β -mercaptoethanol (4%, v/v, HSCH₂CH₂OH, final), and POP6 (0.1%, w/v, final) for suppressing electroendosmosis (15) into a final volume of 1 mL.

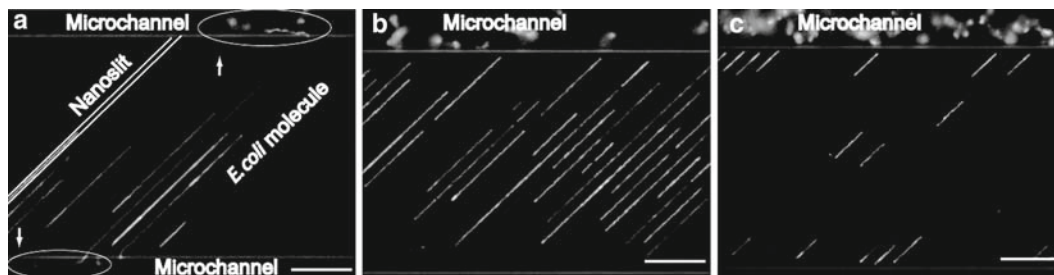


Fig. 2. Gallery of fluorescence micrographs shows stretched and relaxed DNA molecules within the nanoslit device after electrokinetic loading. Relaxed molecules within the microchannel regions appear as diffuse, partly out of focus, fluorescent balls, whereas stretched molecules appear as long linear objects. **(a)** A large *E. coli* DNA molecule spans across the 105- μ m-long nanoslit (0.01 \times TE buffer) showing relaxed ends (*circled*) within abutting microchannels. **(b)** T4 DNA (166 kbp) molecules in 0.05 \times TE buffer. **(c)** λ DNA (48.5 kbp) molecule in 0.01 \times TE buffer. Scale bars = 20 μ m (Reproduced from ref.(16). Copyright 2007 National Academy of Sciences, USA.

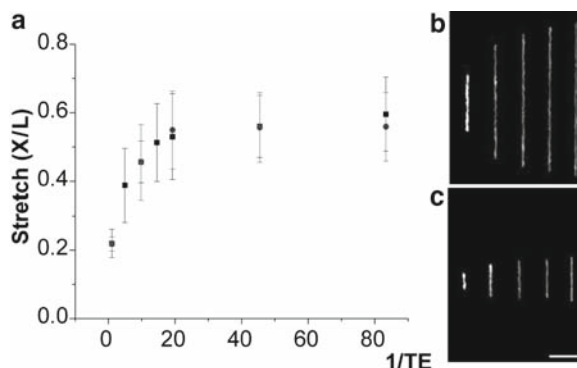


Fig. 3. DNA stretch varies with diluted TE concentration of the λ DNA (open square) and T4 DNA (filled circle). (a) Ionic strength varied through dilutions of Tris-EDTA buffer ($1\times$ TE: 10 mM Tris-base, 1 mM EDTA, pH 8.0). The dilution factors are 1.0, 5.0, 9.8, 14.6, 19.3, 45.5, and 83.5 of $1\times$ TE (ionic strength = 8.5 mM). The stretch is defined by apparent length (X) divided by the polymer contour length (L) of YOYO-1-stained DNA. Each data point represents measurements from 50 to 300 molecules and error bars show standard deviations on the means. (b, c) Fluorescence micrographs (a combination of five separate experiments) show T4 DNA (166 kbp) (b) and λ DNA (48.5 kbp) (c) at five different TE dilutions: 1.0, 9.8, 19.3, 45.5, and 83.5 (dilution factors). Scale bar = 10 μ m (Reproduced from ref. (16). Copyright 2007 National Academy of Sciences, USA.

2. Add DNA sample. In an example in Fig. 3, we add 2 μ L of DNA in $1\times$ TE into 1 mL buffer described in step 1 (see Note 13).
3. Affix a glass coverslip (22 \times 22 mm) with wax on a rectangular opening (18 \times 18 mm) of a Plexiglas slide (25.4 \times 76.2 mm) (see Fig. 1a).
4. Place a PDMS device on this glass window. Press gently to seal the PDMS to the clean glass but take care to not collapse the small features.
5. Load DNA sample into microchannels by capillary loading (see Fig. 1a).
6. Fill the reservoir with the same ionic strength buffer of the DNA sample for electrokinetic loading via the indicated electrodes in Fig. 1a.
7. Place the Plexiglas slide on the table of the fluorescence microscope and focus on the nanoslits.
8. Apply an electric potential (70 V) to transport relaxed DNA coils to nanoslit entrances for subsequent elongation (see Note 14).
9. After turning off the electric field, wait for several minutes for DNA to reach the steady state of relaxation within nanoslits (see Note 15).

3.6. Microscopy and Image Processing

1. Use microscopes equipped with two CCD cameras, that have two filtering optics for green and red colors, respectively (*see Subheading 2.6*). The green channel acquires images of DNA backbone stained with YOYO-1 (491 nm, absorption; 509 nm, emission), and the red channel acquires images of sequence-specific decorations of Alexa Fluor 647 (650 nm absorption; 665 nm emission) punctuates via fluorescence resonance energy transfer (FRET) (*see Note 16*).
2. Flatten images by image-processing software (*see Note 17*).
3. Identify DNA molecules in images by connecting neighboring pixels with fluorescence intensities above a threshold value.
4. Overlap the two corresponding images.
5. Determine molecular size based on integrated fluorescence intensities as well as the end-to-end length.
6. Determine corresponding punctate positions within a molecule using integrated fluorescence intensity profiles and unity based mapping (*see Note 18*).

4. Notes

1. In this case, the ionic strength of 1× TE (10 mM Tris, 1 mM EDTA) is 8.4 mM. On the other hand, typical 1× TE buffer usually starts from EDTA sodium salts and Tris-HCl titrated with NaOH. In this case, the ionic strength is 13.7 mM.
2. Although the width of a nanoslit pattern in the chrome mask is 750 nm, the width of a nanoslit template in a wafer is wider than 750 nm because of light diffraction. The width of a nanoslit can be optimized by adjusting exposure time.
3. A master wafer of nanoslits is dry-etched according to **ref. (20)** instead of a photoresist template built on the wafer like **ref. (17)**. We notice a gradual erosion of the SU-8 photoresist pattern (100-nm height) with the repetition of replica molding; in contrast, an etched silicon wafer master has a higher mechanical stability.
4. Long curing times are critical for stable PDMS nanostructures. With short curing times, 100-nm high PDMS nanoslits often collapse and disappear.
5. PDMS surfaces have a highly polar surface immediately after plasma treatment. If DNA solution is loaded in this reactive PDMS device, a significant amount of DNA molecules will affix to the PDMS device.
6. Without EDTA treatment, fluorescence intensity decreases as DNA molecules travel inside nanochannels. This problem

may be caused by platinum ions, the catalyst for PDMS polymerization, which may cause cyanine dye (YOYO-1) to dissociate from DNA backbones (21, 22). Thus, YOYO-1-stained DNA molecules become dimmer either because the local Pt^{2+} concentration may be high within a nanoslit or because the Pt^{2+} effect is accumulated as DNA traverses a nanoslit. To resolve this issue, sonicating a PDMS device submerged in an EDTA buffer solution extracts platinum ions from PDMS.

7. Commercial coverslips have coating materials that have been added by the glass manufacturer. Thus, the acid cleaning procedure removes coating materials on the glass surface. For safety and cleanliness, a self-contained acid boiling system was built. The main components of this system are made from Pyrex glass cylinders, Teflon tubing, and Teflon sealing "O" rings, all of which are resistant to strong acids. Vacuum grease is not used to seal any joints. Custom Teflon racks were also designed to hold the cover slips securely during the cleaning process.
8. All steps are performed in test tubes and then loaded into the nanoslit device after dilution or dialysis, because the shortage of biochemically meaningful salt concentrations in the nanoslits obviously causes problems for most DNA modification enzymes used for genome analysis.
9. Because preexisting DNA nicks would produce spurious signals, such sites are repaired or disabled using T4 ligase or polymerase incorporation of dideoxynucleotides (ddNTPs) before labeling.
10. Because nick-translation efficiently incorporates fluorochrome-labeled nucleotides, crossing of mobilized nick sites on complementary DNA strands occurs, producing double-strand breaks; this is reduced by the continued presence of ddNTPs in the labeling reaction mix, thus, limiting the number of nucleotides incorporated per nick site through chain termination.
11. The termination of polymerase action by ddNTPs controls the size of fluorescent punctuates, which would otherwise expand into each other if nucleotide incorporation was unchecked, thus, diminishing the number of discrete markers.
12. A nicking enzyme (Nb.BbvCI; GC[^]TGAGG) cleaves only cognate sites on single strands of double-stranded molecules made detectable by nick translation using fluorochrome-labeled nucleotides (23–25).
13. Low ionic strength increases DNA intrachain electrostatic repulsion. DNA molecules could be enlarged in terms of physical measures of size that would hinge on a polymer's persistence length—a characteristic proportional to the

“stiffness” of a chain reflecting the relative directional orientation of several infinitesimal segments. DNA molecules are stretched up to 60% of their polymer contour length in disposable PDMS devices having $100 \times 1,000$ -nm channels under low ionic-strength conditions (*see Fig. 3*); remarkably, these results are comparable to what was previously obtained under standard buffer conditions using 30×40 -nm channels fabricated on fused silica substrates using nanoimprint or electron beam lithography (*14*).

14. DNA molecules electrokinetically progress through the micro-channels as relaxed coils until approaching a nanoslit entrance. There, as one end of a molecule enters the nanoslit, the DNA molecule transiently elongates.
15. DNA molecules expectedly enter nanoslits with different conformations and reach equilibrated forms via different relaxation processes, such as dynamic shrinking and unfolding (elongation).
16. Because labeled DNA molecules are globally stained with the intercalating dye, YOYO-1, we reasoned that fluorescence resonance energy transfer (FRET) would operate between YOYO-1 (FRET donor) and the sequence-specifically placed AlexaFluor-647 labeled nucleotides (FRET acceptor) because they are intimately situated within the same DNA backbone and spectrally compatible. **Figure 5** shows FRET detection of barcode features and their spacing (in kilobases) using integrated fluorescence intensity measurements of the YOYO-1 signals between them.
17. Laser light has a Gaussian shape of light intensity, which generates varying fluorescent intensities for an equivalent amount of fluorochrome. For quantitative analysis, this nonhomogenous fluorescent response should be computationally corrected (*2*).
18. A “unity-based” approach (*1, 5, 26*) uses integrated fluorescence intensity or apparent length for estimation of restriction fragment masses, with the assumption that molecules are not broken. Such measurements were performed on a per fragment basis then normalized by total fluorescence intensity (or size) of the entire molecule, so that the apportionment of fragment fluorescence intensities (or sizes) sums to 1.0. The prevailing assumption generally holds for relatively small DNA molecules (<180 kb) (*27, 28*). Final maps are then constructed by averaging fluorescence intensity measurements of like restriction fragments over a number of molecules, allowing estimation of precision expressed as a standard deviation. Here, we adapt this approach by measuring the integrated fluorescence intensity of intervals, demarcated by fluorescent punctates (*see Fig. 4*).

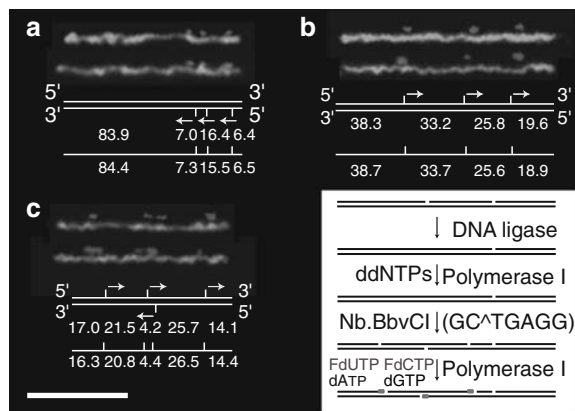


Fig. 4. Molecular barcoding scheme and image gallery of molecules “barcoded” by a nicking enzyme, followed by fluorochrome labeling via nick translation and detection by fluorescence resonance energy transfer (FRET). (*Inset*) First, DNA ligation and nick translation with ddNTPs eliminates or incapacitates inherent nicks on molecules to be barcoded; second, Nb.BbvCI places site-specific nicks on these molecules; and lastly, incorporation of fluorochrome-labeled dNTPs (AlexaFluor 647-aha-dCTP, UTP) nick sites by *E. coli* DNA polymerase I. The fluorescence micrographs of labeled DNA molecules compared with the expected labeling pattern derived from the sequence. (a) BAC79 (113.7 kb), (b) BAC150 (116.8 kb), (c) BAC614 (82.5 kb) with two molecules corresponding in silico map shown per sample. Arrows indicate the direction of nick translation on a given strand. Scale bar = 10 μ m (Reproduced from ref.(16). Copyright 2007 National Academy of Sciences, USA.

Acknowledgments

The authors thank Dr. Dalia M. Dhingra for assisting in the development DNA barcoding, Prof. Theo Odijk for his theory development of DNA elongation within nanoslits, Prof. Juan J. de Pablo and Prof. Michael D. Graham for their advice, and Dr. Guy Plunkett III for bacterial artificial chromosomes and their sequence data. This work was supported by National Institutes of Health Grant 5R01HG000225 and National Science Foundation Grant NSEC DMR-0425880.

References

1. Schwartz, D. C., Li, X., Hernandez, L. I., Ramnarain, S. P., Huff, E. J., & Wang, Y. K. (1993). *Science* **262**, 110–114
2. Dimalanta, E. T., Lim, A., Runnheim, R., Lamers, C., Churas, C., Forrest, D. K., de Pablo, J. J., Graham, M. D., Coppersmith, S. N., Goldstein, S., et al. (2004). *Anal. Chem.* **76**, 5293–5301
3. Zhou, S., Herschleb, J., & Schwartz, D. C. (2007). in *New Methods for DNA Sequencing* ed. Mitchelson, K. R. (Elsevier Scientific Publishers, Amsterdam, Netherland), pp. 265–300
4. Cai, W., Aburatani, H., Stanton, V. P., Jr., Housman, D. E., Wang, Y. K., & Schwartz, D. C. (1995). *Proc. Natl. Acad. Sci. U.S.A.* **92**, 5164–5168
5. Meng, X., Benson, K., Chada, K., Huff, E. J., & Schwartz, D. C. (1995). *Nat. Genet.* **9**, 432–438

6. Valouev, A., Schwartz, D. C., Zhou, S., & Waterman, M. S. (2006). *Proc. Natl. Acad. Sci. U. S. A.* **103**, 15770–15775
7. Valouev, A., Zhang, Y., Waterman, M. S., & Waterman, M. S. (2006). *Bioinformatics* **22**, 1217–1224
8. Lin, J., Qi, R., Aston, C., Jing, J., Anantharaman, T. S., Mishra, B., White, O., Daly, M. J., Minton, K. W., Venter, J. C., et al. (1999). *Science* **285**, 1558–1562
9. Armbrust, E. V., Berges, J. A., Bowler, C., Green, B. R., Martinez, D., Putnam, N. H., Zhou, S. G., Allen, A. E., Apt, K. E., Bechner, M., et al. (2004). *Science* **306**, 79–86
10. Lai, Z., Jing, J., Aston, C., Clarke, V., Apodaca, J., Dimalanta, E. T., Carucci, D. J., Gardner, M. J., Mishra, B., Anantharaman, T. S., et al. (1999). *Nat. Genet.* **23**, 309–313
11. Perna, N. T., Plunkett, G., III, Burland, V., Mau, B., Glasner, J. D., Rose, D. J., Mayhew, G. F., Evans, P. S., Gregor, J., Kirkpatrick, H. A., et al. (2001). *Nature* **409**, 529–533
12. Zhou, S., Kile, A., Bechner, M., Place, M., Kvikstad, E., Deng, W., Wei, J., Severin, J., Runnheim, R., Churas, C., et al. (2004). *J. Bacteriol.* **186**, 7773–7782
13. Cao, H., Yu, Z. N., Wang, J., Tegenfeldt, J. O., Austin, R. H., Chen, E., Wu, W., & Chou, S. Y. (2002). *Appl. Phys. Lett.* **81**, 174–176
14. Reisner, W., Morton, K. J., Riehn, R., Wang, Y. M., Yu, Z. N., Rosen, M., Sturm, J. C., Chou, S. Y., Frey, E., & Austin, R. H. (2005). *Phys. Rev. Lett.* **94**, 196101
15. Tegenfeldt, J. O., Prinz, C., Cao, H., Chou, S., Reisner, W. W., Riehn, R., Wang, Y. M., Cox, E. C., Sturm, J. C., Silberzan, P., et al. (2004). *Proc. Natl. Acad. Sci. U.S.A.* **101**, 10979–10983
16. Jo, K., Dhingra, D. M., Odijk, T., de Pablo, J. J., Graham, M. D., Runnheim, R., Forrest, D., & Schwartz, D. C. (2007). *Proc. Natl. Acad. Sci. U.S.A.* **104**, 2673–2678
17. Duffy, D. C., McDonald, J. C., Schueller, O. J. A., & Whitesides, G. M. (1998). *Anal. Chem.* **70**, 4974–4984
18. Zhou, S., Deng, W., Anantharaman, T. S., Lim, A., Dimalanta, E. T., Wang, J., Wu, T., Chunhong, T., Creighton, R., Kile, A., et al. (2002). *Appl. Environ. Microbiol.* **68**, 6321–6331
19. Reed, J., Singer, E., Kresbach, G., & Schwartz, D. C. (1998). *Anal. Biochem.* **259**, 80–88
20. Effenhauser, C. S., Bruin, G. J. M., Paulus, A., & Ehrat, M. (1997). *Anal. Chem.* **69**, 3451–3457
21. Markstrom, M., Cole, K. D., & Akerman, B. (2002). *J. Phys. Chem. B* **106**, 2349–2356
22. Eriksson, M., Karlsson, H. J., Westman, G., & Akerman, B. (2003). *Nucleic Acids Res.* **31**, 6235–6242
23. Heiter, D. F., Lunnen, K. D., & Wilson, G. G. (2005). *J. Mol. Biol.* **348**, 631–640
24. Xu, S. Y., Zhu, Z., Zhang, P., Chan, S. H., Samuelson, J. C., Xiao, J., Ingalls, D., & Wilson, G. G. (2007). *Nucleic Acids Res.* **35**(14), 4608–4618
25. Xiao, M., Phong, A., Ha, C., Chan, T. F., Cai, D., Leung, L., Wan, E., Kistler, A. L., DeRisi, J. L., Selvin, P. R., et al. (2007). *Nucleic Acids Res.* **35**, e16
26. Jing, J., Reed, J., Huang, J., Hu, X., Clarke, V., Edington, J., Housman, D., Anantharaman, T. S., Huff, E. J., Mishra, B., et al. (1998). *Proc. Natl. Acad. Sci. U.S.A.* **95**, 8046–8051
27. Cai, W., Aburatani, H., Stanton, V. P., Jr., Housman, D. E., Wang, Y. K., & Schwartz, D. C. (1995). *Proc. Natl. Acad. Sci. U.S.A.* **92**, 5164–5168
28. Cai, W., Jing, J., Irvin, B., Ohler, L., Rose, E., Shizuya, H., Kim, U. J., Simon, M., Anantharaman, T., Mishra, B., et al. (1998). *Proc. Natl. Acad. Sci. U.S.A.* **95**, 3390–3395